

## Influence of steel-concrete interaction in dissipative zones of frames: II - Numerical study

Gelu Danku<sup>a</sup>, Dan Dubina<sup>\*</sup> and Adrian Ciutina<sup>b</sup>

*Department of Steel Structures and Structural Mechanics, Faculty of Civil Engineering  
– The “Politehnica” University, Str. Ioan Curea No. 1, Timisoara, Romania*

*(Received October 19, 2012, Revised April 20, 2013, Accepted July 17, 2013)*

**Abstract.** In the case of seismic-resistant composite dual moment resisting and eccentrically braced frames, the current design practice is to avoid the disposition of shear connectors in the expected plastic zones, and consequently to consider a symmetric moment or shear plastic hinges, which occur only in the steel beam or link. Even without connectors, the real behavior of the hinge may be different from the symmetric assumption since the reinforced concrete slab is connected to the steel element close to the hinge locations, and also due to contact friction between the concrete slab and the steel element. At a larger level, the structural response in the case of important seismic motions depends directly on the elasto-plastic behavior of elements and hinges. The numerical investigation presented in this study summarizes the results of elasto-plastic analyses of several steel frames, considering the interaction of the steel beam with the concrete slab. Several parameters, such as the inter-story drift, plastic rotation requirements and behavior factors  $q$  were monitored. In order to obtain accurate results, adequate models of plastic hinges are proposed for both the composite short link and composite reduced beam sections.

**Keywords:** composite beams; plastic hinges; inter-storey drift; numerical models

---

### 1. Introduction

Modern seismic design codes such as EN 1998-1-1 (2003) and P100/1 (2006) allow the Incremental Dynamic Analysis (IDA) as an alternative to the method of equivalent lateral forces. However, the IDA methodology applied to steel and composite steel - concrete frame typology assumes the development of plastic hinges in dissipative zones. The Moment Resisting Frames (MRF) and Eccentrically Braced Frames (EBF) are recognized as structures with a good dissipation capacity, allowing high values of behavior factors  $q$ . Dissipative zones are located in beams, in the case of MRF's, and respectively in links, in the case of EBF's. Consequently, in order to obtain a realistic response from IDA, an adequate behavior is required for plastic hinges and elements.

Various researchers have investigated the response of steel EBF's and dual MRF + EBF frames, but, in most cases, by disregarding the influence of the concrete slab on the overall structural

---

\*Corresponding author, Professor, E-mail: dan.dubina@ct.upt.ro

<sup>a</sup> Ph.D., E-mail: gelu.danku@ct.upt.ro

<sup>b</sup> Associate Professor, E-mail: adrian.ciutina@ct.upt.ro

performance. Chao and Goel (2006) propose a method of design for the EBF steel elements based on target displacement, using the Performance-Based Seismic Design. The numerical investigation conducted by Özhendekci and Özhendekci (2008) shows the difference in terms of elastic and inelastic lateral force distribution in EBF's. The study also shows that, in many cases, the plasticization of EBF links is concentrated on a limited number of storeys. Bosco and Rossi (2009) present an interesting numerical work by considering the steel link modeled by three resorts. The authors define a new parameter, called *damage distribution capacity factor* and use it in order to characterize the seismic response of EBF structures. Degee *et al.* (2010) present a parametrical numerical study concentrated on EBF's with vertical short steel links working in shear and composite beams, by using nominal material characteristics. Although the main aim of the study is focused on the influence of material variability over the seismic response of structures, partial conclusions show a good behavior of the vertical steel links conducting to behavior factors close to 6, although a smaller factor was used or design.

Concerning the plastic response of composite beams in MRF, Nie and Tao (2012a) investigated the main factors that affect the resistance of the beam end-section in negative bending. The study shows that the column width, the beam height and the flange width may influence the negative effective width of beams and hence its resistance. The study is completed through investigation on 10-story structures subjected to seismic lateral loading (Nie and Tao 2012b). The authors show that the neglect of the spatial composite effect of the slabs may lead to unsatisfactory predictions in terms of lateral stiffness of frames.

Preliminary tests performed on steel dual MR+EBF (Ricles and Popov 1987, Danku 2011), with the steel beams connected to the concrete slab (composite beams) show that the composite effect has a favorable influence on the resistance of the plastic hinge, while maintaining the high ductility of the systems. Also, the disconnection of steel elements from the concrete slab does not assure a similar behavior with the steel element alone, but is more close to a full-connection situation.

The study focuses on investigating the response of MRF and EBF (including dual configuration) with composite beams through advanced engineering checking, including IDA with accelerograms. The methodology is based on the calibration of the numerical model, both for plastic hinges and elements.

## 2. Behavior of plastic hinges

The plastic hinges act as fuses in dissipating seismic input energy through elastic-plastic cycles in bending (for MRF) and shear (for EBF). In current practice, the model defining plastic hinges only involves the use of the steel section in order to define plastic behavior. When considering steel beams composite with the concrete slab, the general tendency is to avoid the connection over the dissipative zone, thus allowing the plastic hinge to fully develop in the steel profile.

A common solution for concentrating the plastic hinge in a desired position is by using Reduced Beam Section (RBS), usually on the beam, in the vicinity of the beam-to-column joint (Plumier 1990). It implies the reduction of beam section by flange cutting. The procedure is also applied to prevent premature failure of the joint or column panel.

The experimental results obtained on dissipative zones of MRF and EBF and described in the joint article *Influence of steel-concrete interaction in dissipative zones of frames: I - Experimental Study* are used as a basis for the calibration of plastic hinge behavior in order to consider the

composite effect on the plastic behavior of the element. They will be further used in nonlinear analyses (time-history, pushover) on larger frames.

The computer code SAP2000 (CSI 2012) was considered as a rational design tool for the required analysis. A parameter in the choice of the analysis software was the large distribution among the steel design engineering community. The hinge definition module developed in version 14 in SAP2000 computer code allows for the definition of various plastic hinge properties, such as:

- M3 bending hinge, usually assigned to elements (e.g., beams) - user specifications allowed;
- V2 shear hinge – assigns a hinge to an element working in shear (e.g., short links), - user specifications allowed;
- P axial hinge type can be applied to axially loaded elements, such as braces. Different hinge properties may be defined in tension and compression;
- P-M2-M3 – axial and biaxial bending moment hinge, used for the modeling of the plastic behavior of columns.

These models are mostly used for steel sections and are symmetric in behavior by implicit definition (see Fig. 1). The model for the plastic hinge includes only the definition of the plastic curve through rigid-plastic behavior, while the elastic behavior is integrated in the element model. Different key-points can define plastic deformations related to Immediate Occupancy (IO), Life Safety (LS) and Collapse Prevention (CP) limit states.

However, the implementation and use of a plastic hinge model for composite cross-sections, requires good knowledge on the elasto-plastic behavior of the structural elements and joints including the influence of alternate loads.



Fig. 1 Example of default plastic hinge definition in SAP2000 (SAP 2000, 2012)

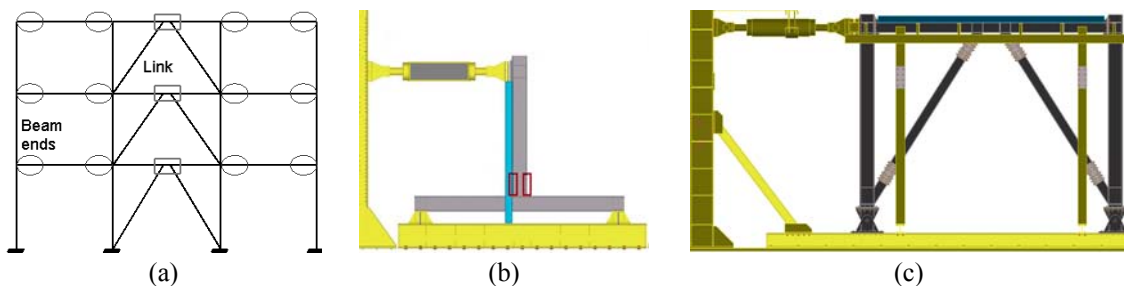


Fig. 2 (a) Dissipative zones for MRF + EBF dual configuration; (b) testing set-up for DB; and (c) EBF specimens

A realistic plastic behavior of a hinge is obtained through the definition of the key points that follow the behavior resulted from experimental envelope curves. Experimental tests focused on the behavior of dissipative zones of dual MRF + EBF (see Fig. 2(a)). The testing set-ups of the beam-to-column and EBF specimens are shown in Fig. 2 – middle and right, respectively. Thus, the three-linear curves with descending branch shown in Fig. 3 were derived on the basis of the experimental envelope curves obtained for bending and shear elements.

However, the experimental results show a significant difference between the behavior of pure steel and the composite (both connected or not over the hinge) for all the monitored parameters: resistance, initial rigidity and ductility. Consequently, the plastic-hinges defined for the composite cross-sections should be asymmetrical, with distinct behavior for positive and negative branches. Fig. 3 shows graphically the definition of the key points chosen for the plastic hinges characteristic curves for RBS (moment – rotation) and short EBF links (shear force – distortion) respectively with respect to FEMA recommendations for IO, LS and CP limit states (FEMA 2000). The quadric-linear numerical models shown in Fig. 3 were chosen so as to follow the experimental results very closely.

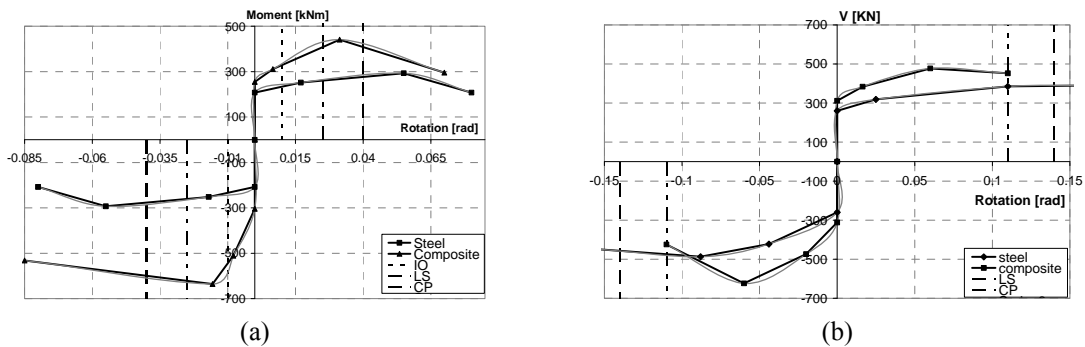


Fig. 3 (a) Plastic hinges developed in the RBS; and (b) link for steel and composite specimens

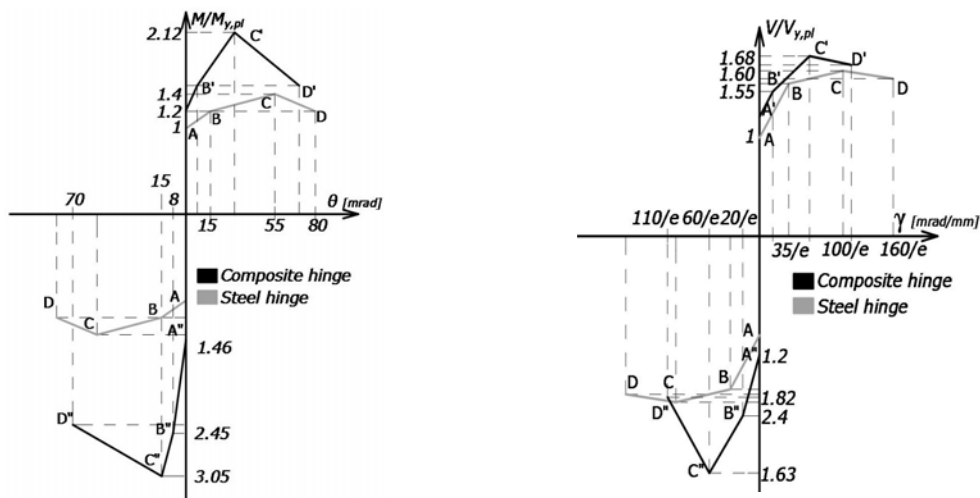
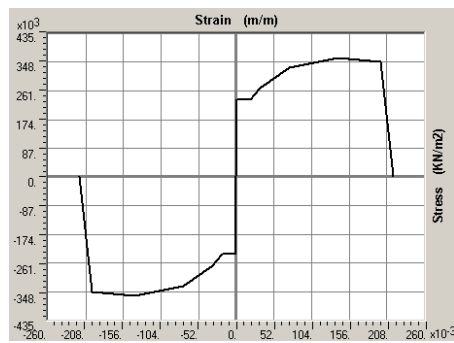


Fig. 4 Normalized definition of moment and shear hinges

Considering the characteristics for the steel and composite beam and link hinges, the key-points definitions could be normalized as in Fig. 4, taking as unity the plastic resistance of steel elements: in bending for RBS of beams, and, respectively, in shear for short links.

The hinge behavior was validated by integrating its characteristic curve into numerical models, along with the simulation of the tested specimens (presented in Fig. 2): experimental EBF (EBF\_M\_LF-M specimen) and the beam-to-column joint (DB-C\_RLD specimen), respectively. In order to obtain accurate models, the real stress-strain material definitions were used for elements, as they resulted from traction tests on samples. Multi-linear elastic-plastic material models were used with the nominal characteristics given in Fig. 5.

The lateral force versus top displacement curve resulted from numerical simulations show good agreement with the experimental response for both joints (DB specimens) and link (EBF specimens), as shown in Fig. 6. However, in case of EBF simulations it was necessary to replicate the slip in the brace connections through elastic link elements, in order to obtain good accuracy of the initial rigidity of the frame. This considered a linear relationship between force and displacement, a 5 mm slip corresponding to an axial load of 800 Kn.

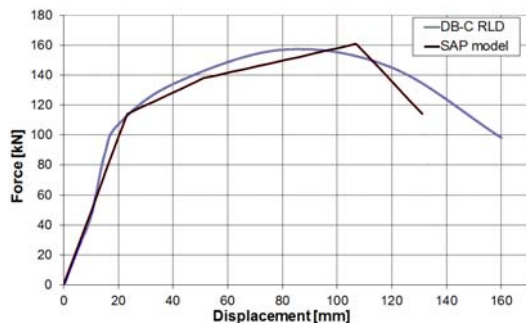


Steel grade S235 - isotropic  
 $E = 210000 \text{ N/mm}^2$   
 $f_y = 235 \text{ N/mm}^2$   
 $f_u = 360 \text{ N/mm}^2$

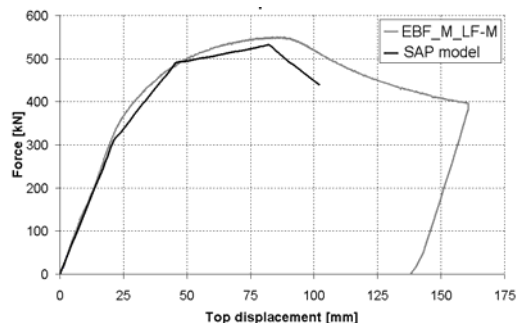


Steel grade S355 - isotropic  
 $E = 210000 \text{ N/mm}^2$   
 $f_y = 355 \text{ N/mm}^2$   
 $f_u = 510 \text{ N/mm}^2$

Fig. 5 Material definition for steel grades S235 (beams) and S355 (columns and braces)



(a)



(b)

Fig. 6 Experimental versus numerical lateral force – top displacement relationships for DB and EBF specimens respectively

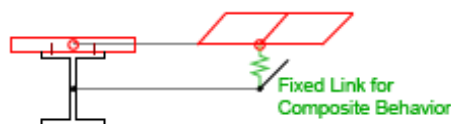


Fig. 7 Numerical model used for simulation of composite beams (SAP 2000)

### 3. Calibration of composite response for beams

The numerical response of composite steel and concrete beams represents a delicate matter due to the difficulty of assessing differences between material properties, both in the elastic and plastic range – rigidity, resistance and deformation to failure / crushing etc. The frame modeling of such elements is even more complicated due to the concentration of sectional properties on longitudinal elements (Zona *et al.* 2000). Elghazouli *et al.* (2008) shows that a fiber model for composite beam section with discrete links simulating the connection between the steel and the concrete elements can simulate good composite behavior. However, the behavior of joints should be foreknown. Vasdravellis *et al.* (2009) show that partial connection between the steel beam and the concrete slab could be modeled with good accuracy by considering for each connector a special finite element in advanced computer codes such as ABAQUS.

Other research-dedicated software such as Open SEES (2012) or DRAIN 2/3DX (2012), used for modeling composite cross sections in frames analysis, use fiber models with different material characteristics for structural steel, concrete and reinforcement. However, these programs are difficult to use in the actual process of design.

The SAP2000 computer software, version 12.0, allows for several models for composite elements. The model chosen in order to simulate the composite beam has been adapted according to the one proposed at CSI Berkeley in April 2010, and first implemented in SAP2000, version 12.0. This has proven to work adequately by comparing numerical and analytical results, for simple cases of simply-supported and double-encased beams. The model uses a bar element for the steel profile and a shell element, in order to simulate the concrete layer, while a fixed link is used as connection between steel and concrete. The steel frame element and shell are drawn at the elevations of their centroids, while the connection is made at fixed intervals (see Fig. 7).

Composite beams behavior was calibrated through push-over analysis on composite joint (DB\_Comp\_RLD) and EBF (EBF\_LF2\_Comp\_C1) subassemblies, by direct comparison between experimental and numerical results. The subassemblies are part of a composite DUAL MRF+EBF structure (see Fig. 2) with 4.5 m spans for EBF and 6m spans for MRF. The concrete slab considered a 12 cm thickness and two longitudinal reinforcement layers ( $\Phi$  12 mm distanced at 15 cm), according to the characteristics of experimental tests. The considered slab width for both MRF and EBF, namely 120 cm, was greater than the one required by Eurocode 8 ( $2 \times 0.1 L$ ) and Eurocode 4 ( $2 \times L_0 / 8$ ), in the case of MRF. However, this value is close to  $L/4$ , which is considered by Huang *et al.* (2012) as appropriate for an accurate response of composite frames. Due to the relatively small differences, recorded experimentally, between the composite specimens with and without studs over the dissipative zones, in the calibration process and further analyses there were considered only the composite models without studs over the dissipative zones.

The concrete material behavior was defined based on the results obtained under standard compressive testing on cube samples, and further using the Mander model (CSI 2012), as shown in Fig. 9.

During the experimental tests the dedicated transducers recorded no slip between the slab and the top flange, even for large top displacements. Thus, in numerical simulations, a complete interaction was modeled in longitudinal shear between steel and concrete, without slip. For this purpose, links were placed at a maximum distance of 30 cm from one other, discontinued over the dissipative zones. This distance resulted as adequate, after modeling the complete interaction. The shell element section considered multi-layered non-linear elements, with the concrete represented by the shell layer, and the reinforcements represented by two membrane layers with elastic-plastic behavior. The concrete slab mesh was modeled by two sizes, as follows: a larger mesh of  $15 \times 15$  cm was used for spans with no plasticization expected, while, in the potentially plastic region, a finer mesh ( $2.5 \times 6$  cm) was considered (see Fig. 8).

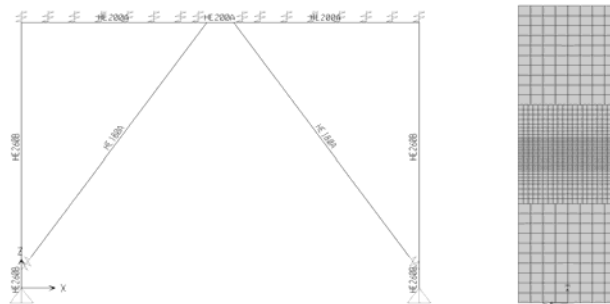
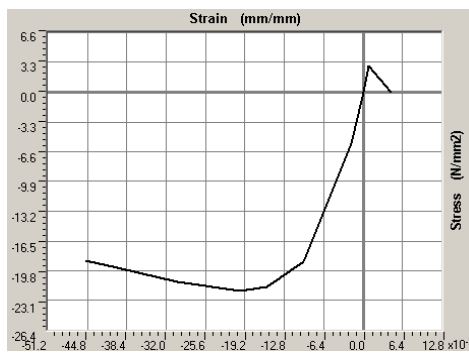


Fig. 8 Finite element model used for the calibration frame



Concrete material definition  
 Concrete class C20/25 – isotropic  
 $E = 30000 \text{ N/mm}^2$   
 $f_{ck} = 22 \text{ N/mm}^2$

Fig. 9 Numerical model used for simulation of concrete material in composite beams

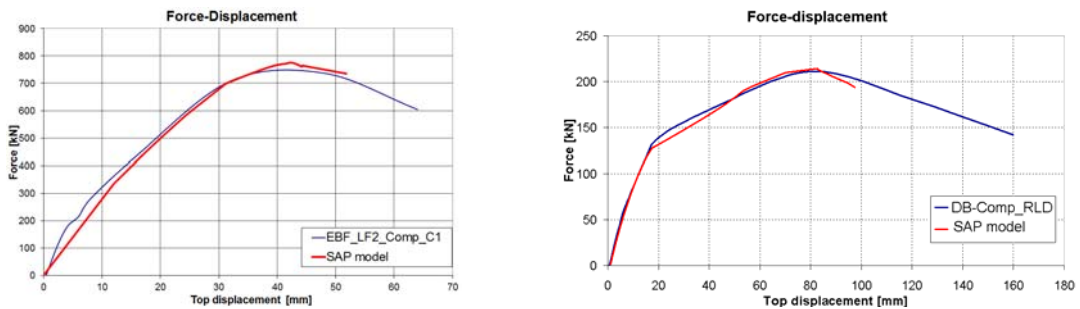


Fig. 10 Experimental and numerical push-over curves obtained for EBF and DB subassemblies

The behavior of the hinges (joints, including beam ends and links) were integrated into the structural response on the basis of the calibrations made in Section 2 and shown in Figs. 3 and 4. Close models of the experimental response were considered. The comparison between numerical and experimental results is given in the form of force – top displacement curves, in Fig. 10, and it proves an accurate response of numerical models for both EBF and DB specimens.

#### 4. Numerical analyses of structures

The numerical investigation consisted in monitoring the nonlinear response of eight 2D structures, designed according to current European seismic regulations. The structures were considered with steel columns, while the beams were designed in two distinct ways, namely steel and composite, thus resulting a total number of 16 structures. The systems considered for analysis were three EBF's, two MRF's and three dual EBF+MRF structures. The study considered a wide variety of structures, from low-rise 4 story structures to 8 and 12 story configurations.

##### 4.1 Details of structural design

Structural elements were designed according to Eurocode 3 (EN 1993-1-1-2006), Eurocode 4 (EN 1994-1-1-2004) and further adapted so as to satisfy the Eurocode 8 (EN 1998-1-1-2004) conditions. The gravitational loads considered were uniformly distributed on floors: dead load - 4 kN/m<sup>2</sup>, live load -3.5 kN/m<sup>2</sup> (including partition walls).

Masses were computed according to the seismic combination 1.0G + 0.3Q and concentrated in structural joints. For the seismic design, an equivalent elastic spectral analysis was performed. The spectrum considered is characteristic to the city of Bucharest, and has the control period  $T_c=1.6s$  and the peak ground acceleration  $a_g = 0.24 g$ . The value of the  $q$  factor was taken as 6 (Table 6.2 from Eurocode 8), corresponding to high ductility class structures. Non-ductile elements were designed by considering the values of  $1.1\gamma_{ov}\Omega$  as 2.5 for EBF and dual frame and 3.0 for MRF. The analyzed structural configurations are given in Fig. 11. All frames are façades, isolated from hypothetical square structures. Notations for different elements are given, depending on their structural typology. The description of spans and element sections is given in Table 1. In order to optimize the seismic structural response, the element cross-section variation was considered on higher levels. However, in the case of MRF beams, the design was performed based on gravitational combination, which leads to the same element section over the entire frame height.

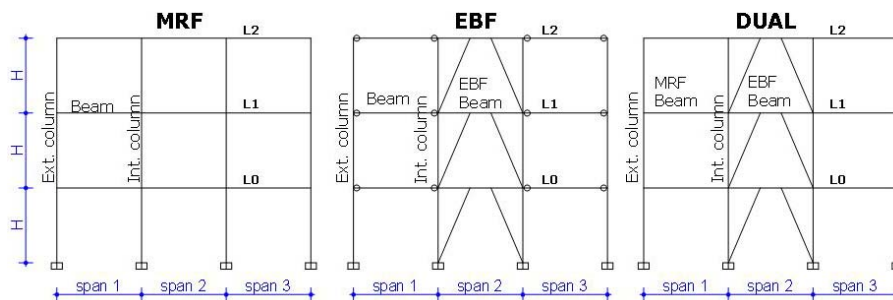


Fig. 11 Lay-out and notations for frames

Table 1 Main data for the analyzed frames

Frame number	Frame name	Nr. of levels	Level Height [m]	Spans [m]	MRF beams	EBF beams	Composite beams	Columns	Braces
F1S	DUAL – 4S	5	4, 4×3.5	8, 6.5, 8	IPE450	IPE360	No	HE400B	L0-L1: HE200B L2-L4: He180B
F1C	DUAL – 4C	5	4, 4×3.5	8, 6.5, 8	IPE450	IPE360	Yes	HE400B	L0-L1: HE200B L2-L4: He180B
F2S	EBF – 4S	5	4, 4×3.5	8, 6.5, 8	IPE400	L0: HE240A L1: HE260A L2: HE240A L3: HE220A L4: HE200A	No	ext: HE300B int: HE400B	L0-L3: HE200B L4: HE180B
F2C	EBF – 4C	5	4, 4×3.5	8, 6.5, 8	IPE400	L0: HE240A L1: HE260A L2: HE240A L3: HE220A L4: HE200A	Yes	ext: HE300B int: HE400B	L0-L3: HE200B L4: HE180B
F3S	DUAL – 8S	9	3.5	7, 6, 7	HE280A	L0-L2: HE300A L3-L4: HE280A L5: HE260A L6-L8: HE220A	No	ext: HE400B int: HE500M	L0-L5: HE240B L6-L8: HE200B
F3C	DUAL – 8C	9	3.5	7, 6, 7	HE280A	L0-L2: HE300A L3-L4: HE280A L5: HE260A L6-L8: HE220A	Yes	ext: HE400B int: HE500M	L0-L5: HE240B L6-L8: HE200B
F4S	EBS – 8S	9	3.5	7, 6, 7	HE280A	L0-L2: HE300A L3-L4: HE280A L5: HE260A L6-L8: HE220A	No	ext: HE400B int: HE500M	L0-L5: HE240B L6-L8: HE200B
F4C	EBS – 8C	9	3.5	7, 6, 7	HE280A	L0-L2: HE300A L3-L4: HE280A L5: HE260A L6-L8: HE220A	Yes	ext: HE400B int: HE500M	L0-L5: HE240B L6-L8: HE200B
F5S	EBS – 6S	7	3.5	7, 6, 7	HE280A	L0-L2: HE300A L3-L4: HE280A L5: HE260A L6: HE220A	No	ext: HE360B int: HE450M	HE200B
F5C	EBS – 6C	7	3.5	7, 6, 7	HE280A	L0-L2: HE300A L3-L4: HE280A L5: HE260A L6: HE220A	Yes	ext: HE360B int: HE450M	HE200B
F6S	DUAL – 12S	13	3.5	6, 6, 6	IPE400	L0-L2: IPE400 L3-L5: IPE360 L6-L8: IPE330 L9: IPE300 L10: IPE270 L11-L12:	No	ext: HE450B int: HE450M	L0-L2: HE300A L3-L5: HE260A L6: HE240A L7-L9: HE220A L10-L11: HE200A

Table 1 Continued

F6C	DUAL – 12C	13	3.5	6, 6, 6	IPE400	L0-L2: IPE400 L3-L5: IPE360 L6-L8: IPE330 L9: IPE300 L10: IPE270 L11-L12:	Yes	ext: HE450B int: HE450M	L0-L2: HE300A L3-L5: HE260A L6: HE240A L7-L9: HE220A L10-L11: HE200A
F7S	MRF – 5S	6	3.5	7.5, 7.5, 7.5	IPE500	-	No	HE600B / HE600M	-
F7C	MRF – 5C	6	3.5	7.5, 7.5, 7.5	IPE500	-	Yes	HE600B / HE600M	-
F8S	MRF5 – 6S	6	3.5	6, 6, 6	IPE400	-	No	HE500B / HE500M	-
F8C	MRF6 – 5C	6	3.5	6, 6, 6	IPE400	-	Yes	HE500B / HE500M	-

\* Note: The design considered the dissipative elements (beams and links) made of the steel grade S235, while the non-ductile elements (EBF braces and columns) made of S355 steel grade. The only exception is the 8 stories frames F4S/C for which the EBF beams were made of S355 steel grade

#### 4.2 Monitored results

The non-linear response of structures was monitored through push-over and incremental dynamic analyses with accelerograms.

The push-over analysis gives valuable information concerning the non-linear response of structures. For the numerical study, the non-linear push-over analyses were used for the confirmation of the plastic failure mechanism considered in design, and also in order to verify whether the structures can reach the target displacements for serviceability and ultimate limit conditions. The N2 method (Fajfar 2000) was used for this verification.

The Incremental Dynamic Analyses (IDA) were used for a complete characterization of the non-linear structural response. Seven earthquakes were considered, all of them recorded from Vrancea source. Details on these recordings could be found elsewhere (Danku 2011):

- One recording from the 1977 Vrancea earthquake (INCERC N-S);
- Three recordings from the 1986 Vrancea earthquake (INCERC N-S, EREN 10W and Magurele N-S);
- Three recordings from the 1986 Vrancea earthquake (INCERC N-S, Magurele N-S and Armeneasca S3E).

The recordings were scaled initially on the design peak ground acceleration corresponding to Bucharest's seismic conditions ( $a_{gdesign} = 0.24$  g). The intensities were then increased up to the reaching of a failure point by an acceleration multiplication factor ( $\lambda$ ).

The failure (ultimate) criteria for the analyzed frames were considered at the reaching of one of the following points:

- Development of a structural mechanism;
- The maximum rotation capacity in a hinge (according to FEMA356);
- The maximum allowable inter-story drift limit (3% were considered as the limiting criterion).

The IDA results show the realistic behavior of structures, indicating the structural response under severe ground motions and the dissipation capacity of the structure. Several parameters were monitored:

- the inter-storey drift values for different limit state conditions, such as serviceability (0.12 g) and ultimate (0.24 g). The inter-storey drifts were expressed as percentages of storey heights: 0.8% for serviceability (SLS) and 2.5% for ultimate (ULS) limit states respectively, according to Eurocode 8 criteria;
- the plastic rotations developed in dissipative elements for different levels of ground acceleration (ultimate and serviceability). Their values were compared to norm conditions and experimental results;
- the behavior factor, expressed as the ratio between the ground motion intensity corresponding to failure ( $\lambda_u$ ) and the multiplier corresponding to the development of the first plastic hinge ( $\lambda_1$ ):  $q = \lambda_u / \lambda_1$ .
- the efficiency of the building  $\eta$ , defining the ability of the structure to withstand a certain earthquake, was computed by  $\eta = a_{gu} / a_g$  (ultimate for design ground accelerations). As the accelerograms were scaled to  $a_g$ , the efficiency is equal to the multiplier of the accelerograms under ultimate conditions:  $\eta = \lambda_u$ .

Elements were modeled considering the elastic-plastic behavior of materials, and the plastic hinges definitions described in the second section.

#### 4.3 Response of the 9 storey DUAL structure

The 9 storey DUAL frame is considered as a typical structure that combines the advantages of MRF and EBF for a convenient height. The convention of rotations shown in Fig. 12 was used for representing damage in structural elements. The values are related to the maximum rotation reached in experimental investigations for link elements in EBF and in RBS in MRF. The red color indicates the results obtained by structures with composite beams, while blue depicts the results obtained with steel beams.

Fig. 13 presents the development of the plastic hinges resulted from the push-over analysis for different levels of top lateral displacement: 90 mm (situation corresponding to the serviceability seismic intensity); 180 mm and 230 mm displacement, corresponding to ultimate limit state conditions. As it could be noted, first plasticization occurred in the lower-level links while the MRF beam ends (RBS) plastify for higher displacements in RBS zones (hogging bending only).

Link hinge	Rotation [mrad]				Max. Value	RBS hinge	Rotation [mrad]				Max. Value
Pattern					166 mrad	Pattern					85 mrad
Steel	0-40	40-110	110-150	>150		Steel	0-15	15-55	55-80	>80	
Pattern					115 mrad	Pattern					80 mrad
Composite	0-15	15-60	60-110	>110		Composite	0-5	5-30	30-70	>70	

Fig. 12 Levels of response rotation for links and RBS

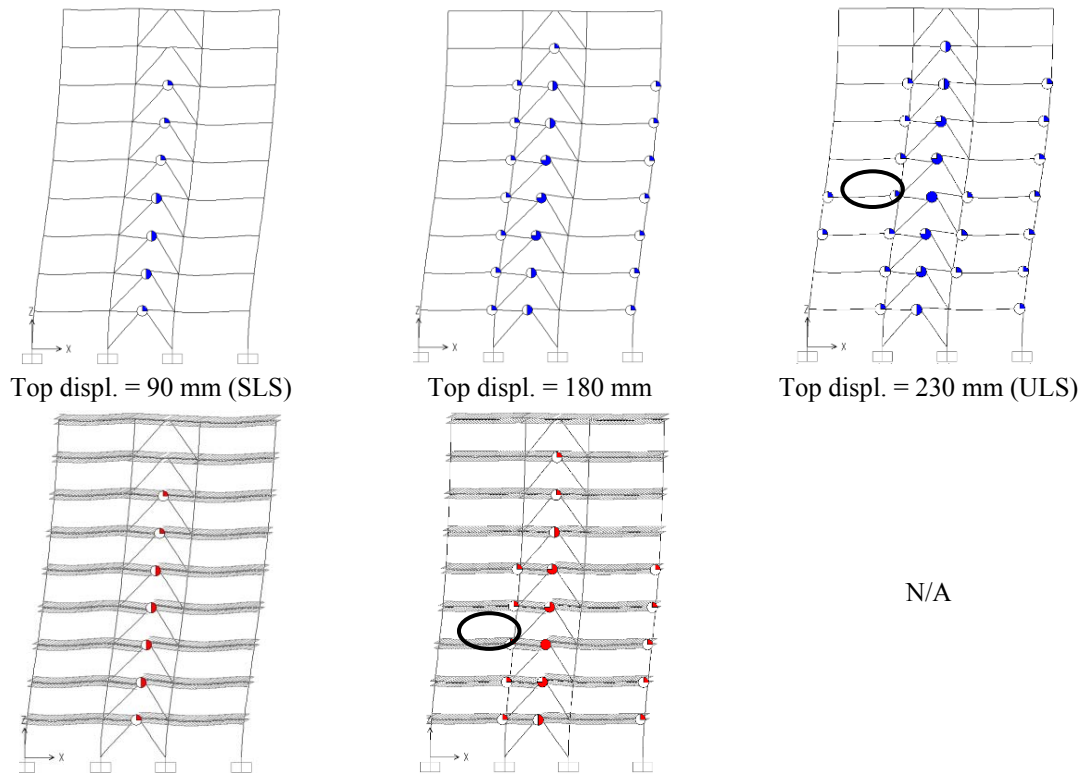


Fig. 13 Push-over response of a nine-storey structure

In both cases (steel and composite), the SLS deflection conditions are reached by plastic hinges formed only in link elements. The ultimate limit state corresponds to the exhaustion of rotation capacity of links, recorded in the mid-stories. It is to be noted that, at the ULS stage, the RBS only have initial plasticization under bending. Thus, a replacement of the EBF link element may restore the building in a recovery state after a strong seismic motion. In the case of composite beams, plastic hinges tend to develop later and have smaller rotation values. Consequently, the composite solution leads obviously to a stiffer structure. Therefore, the structure with composite beams does not reach its target displacement at ULS. Although, the overall performance of the structure with composite beams is appreciated as satisfactory, no damage occurs in non-dissipative elements.

Fig. 14 presents the results of dynamic analyses performed on the DUAL-8 M(C) structures, for design purposes in the case of the 1977 Vrancea INCERC N-S accelerogram. Among the seven accelerograms considered, Vrancea 77 ground motion is the most destructive. The accelerogram was scaled so as to correspond to the peak ground acceleration of 0.24 g ( $\lambda = 1.0$ ) used for design. The charts given in Fig. 13 present the maximum values (envelopes) recorded during the quake action for the RBS rotation, the link distortion, as well as the inter-story drift (expressed as a percentage of the storey height), for each storey respectively.

The largest inter-story drift is recorded at the second level, but the maximum value (roughly 2%) does not exceed the limit given by P100/2006 and Eurocode 8. The stiffer character of the composite frame leads in this case to a maximum drift of about 75% of the one of steel. The link

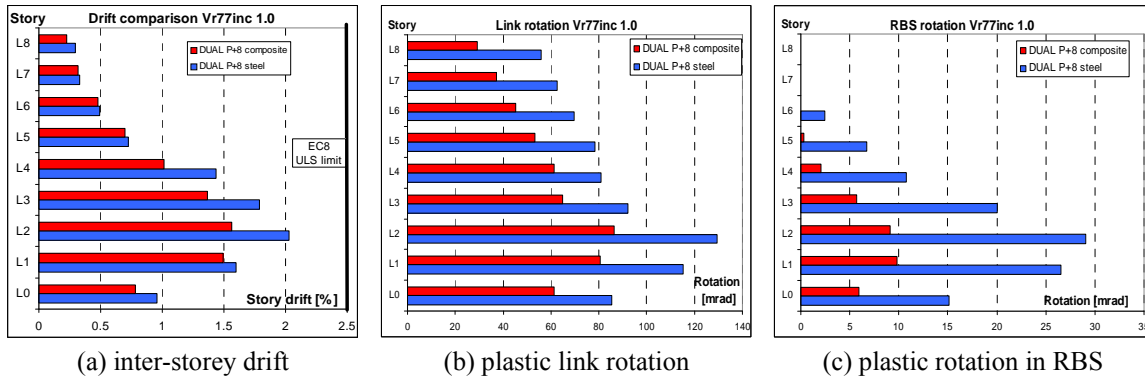


Fig. 14 Maximum values recorded for Vrancea 77 accelerogram

show high ductility, reaching rotation values of 110 mrad for steel and 80 mrad for the composite structure, respectively. The plastic hinge formation in RBS was recorded after the formation of plastic hinges in link elements. The development of hinges in RBS was up to the sixth floor in the steel configuration and fifth floor in the case of composite frames. However, in this case, values are noticeably higher for the steel beams than the composite ones.

Fig. 15 illustrates the difference between the SLS and ULS conditions for the same parameters: envelope inter-storey drift and plastic rotations in link elements and RBS zones. The SLS condition is defined by a half design ground acceleration ( $\lambda = 0.5$ ). The results at SLS show very small differences between the steel and the composite frames, in what concerns the drift values and the RBS zone rotation. However, for lower levels in the structure, there are significant differences in terms of link rotations: 20 mrad for composite, up to 40 mrad for steel frame, respectively. The stiffer character of the composite frame is preserved.

Figs. 16 and 17 present the same recorded parameters under ultimate limit state conditions, for all seven accelerograms. The values of rotations recorded in plastic hinges of links for the composite structure appear to be more evenly distributed along the building height. Considering

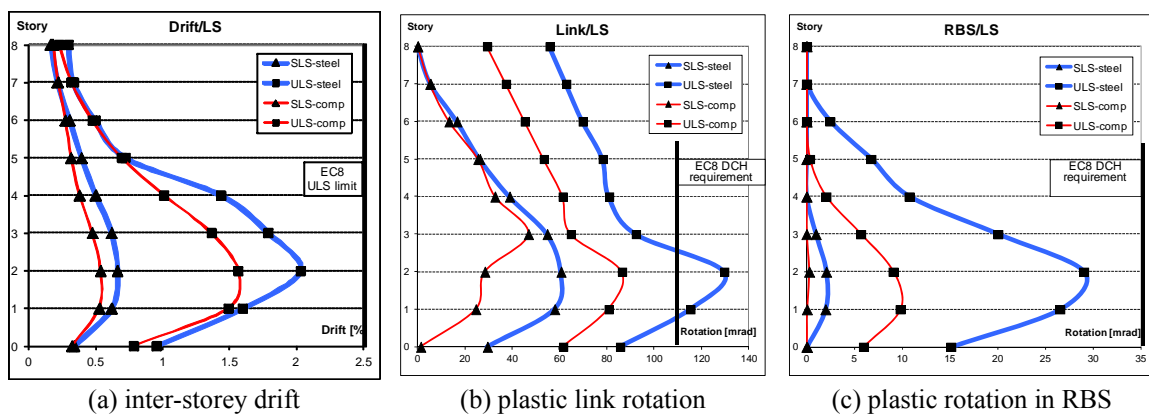


Fig. 15 Differences in SLS and ULD conditions for the 1977 Vrancea accelerogram

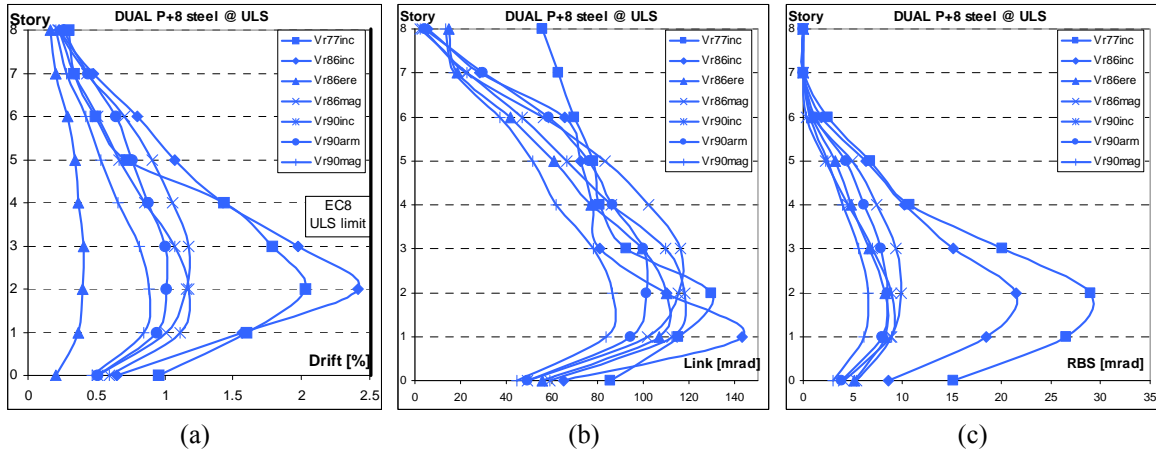


Fig. 16 Results recorded at ULS for steel DUAL 8S frame

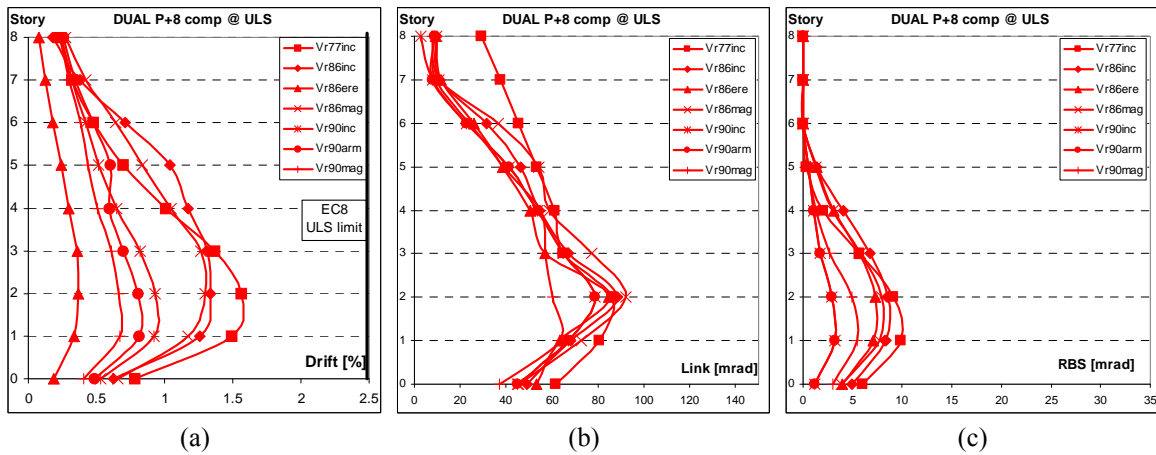


Fig. 17 Results recorded at ULS for composite DUAL 8C frame

the norm limitations for drift and plastic rotation at ULS, the composite structure may be considered as safe, with all the required values for drift and rotations under the norm limiting values. This is also valid in the case of steel frames, with only two exceptions: the link distortion for Vrancea 1977 and 1986 exceeds the required experimental value of 110 mrad. As a general conclusion, it should be noticed that the plastic rotations demands in the case of composite frames is significantly smaller than in the case of steel frames.

#### 4.4 Incremental dynamic analysis results

The results of IDA are presented in the form of charts, by plotting the accelerograms multiplier ( $\lambda$ ) against the top inter-story drift (envelope value). Fig. 18 shows the comparison between the global responses of the 8 story structure in the steel and composite beams solution under seven earthquake recordings from the Vrancea source. The IDA was performed by step-by-step

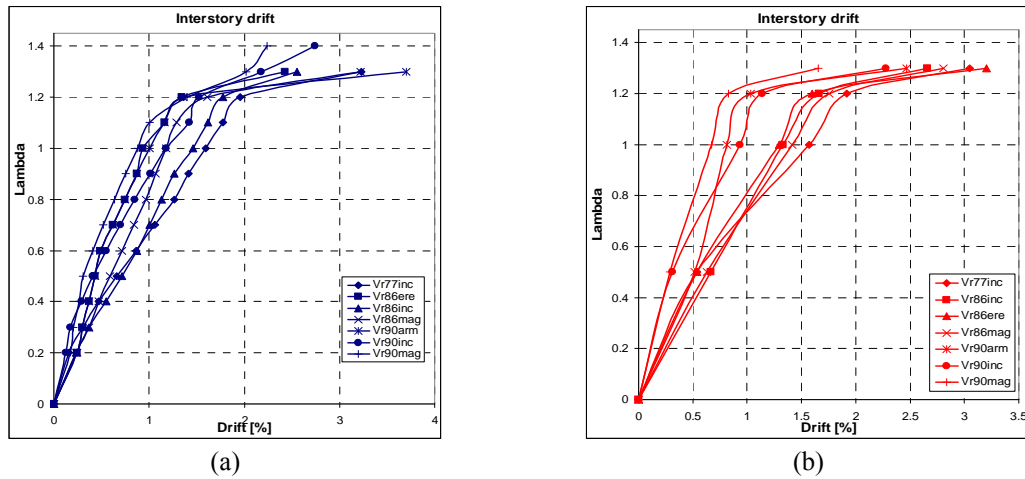


Fig. 18 IDA response representations for the DUAL 8 story steel and composite structure, respectively

incrementation of the acceleration level, while monitoring the top displacement value up to the point when a failure criterion was reached (see Section 4.2). The appearance and development of plastic hinges was also monitored.

The results very clearly show that, in the case of a frame with steel beams, the first plastic hinges are formed at smaller values of  $\lambda$  multipliers than in the case of frames with composite beams, while the failure increment (either by reaching of the failure mechanism or reaching of the maximum rotation in one of the hinges) has similar values. On the other hand, the steel structure shows higher seismic overstrength factors, with a safety reserve of at least 20% ( $\lambda = 1.2$ ). From this point on, deformations for both structures tend to amplify.

#### 4.5 Differences in response: EBF and DUAL structures

The difference in seismic design of EBF and DUAL EBF + MRF is made by the presence of the moment-resisting structure, which has to withstand a lateral seismic force proportional to its stiffness (clause 6.10.2 of Eurocode 8). Consequently, it is to be expected that a dual configuration will be stiffer than the equivalent EBF. Table 2 presents in comparison the drift and rotation requirements for the two types of structures, in the design situation ( $\lambda = 1.0$ ) for each earthquake recording. Also, in Fig. 19 presents the IDA top-drift versus  $\lambda$  multiplier curves for three selected accelerograms. The results show that not in all cases the DUAL structures are stiffer than EBF frames, and, generally speaking, other parameters, such as the shape of the spectrum, govern the particular behavior of the frame. Also, it can be noticed that, in both cases, the inter-storey drift, link distortion and the RBS rotation are smaller for the composite configuration, thus confirming the conclusions drawn up to this point.

#### 4.6 Investigation on behavior factor and seismic efficiency

Table 3 shows the values of  $q$  (behavior factor) and  $\eta$  (seismic efficiency) computed as described in Section 4.2. The results are given for six representative frames. Due to the fact that the accelerograms used in analyses were initially pre-scaled to the design seismic intensity, the  $\eta$

Table 2 Comparison in monitored parameters for EBF and DUAL 8 structures

Results at ULS for EBF – 8 structure						
Quake	Drift requirement [%]		Link rotation [mrad]		RBS rotation [mrad]	
	Steel	Composite	Steel	Composite	Steel	Composite
Vr77inc	1.52	1.27	146	110	---	---
Vr86inc	1.47	0.92	136	96	---	---
Vr86ere	1.36	0.85	125	61	---	---
Vr86mag	1.21	0.72	108	64	---	---
Vr90inc	1.03	0.93	92	53	---	---
Vr90arm	0.97	0.93	85	58	---	---
Vr90mag	0.83	0.53	72	59	---	---

Results at ULS for DUAL – 8 structure						
Quake	Drift requirement [%]		Link rotation [mrad]		RBS rotation [mrad]	
	Steel	Composite	Steel	Composite	Steel	Composite
Vr77inc	1.59	1.56	129	86	29	9
Vr86inc	2.41	1.89	143	128	21	7
Vr86ere	1.11	1.04	110	92	8	7
Vr86mag	0.70	0.62	116	98	9	7
Vr90inc	1.17	0.93	117	110	8	4
Vr90arm	1.00	0.81	101	91	8	3
Vr90mag	0.88	0.66	86	79	6	5

\* Note: all steel beams in DUAL configuration were designed using steel quality S235, while all beams in EBF configuration are steel quality S355

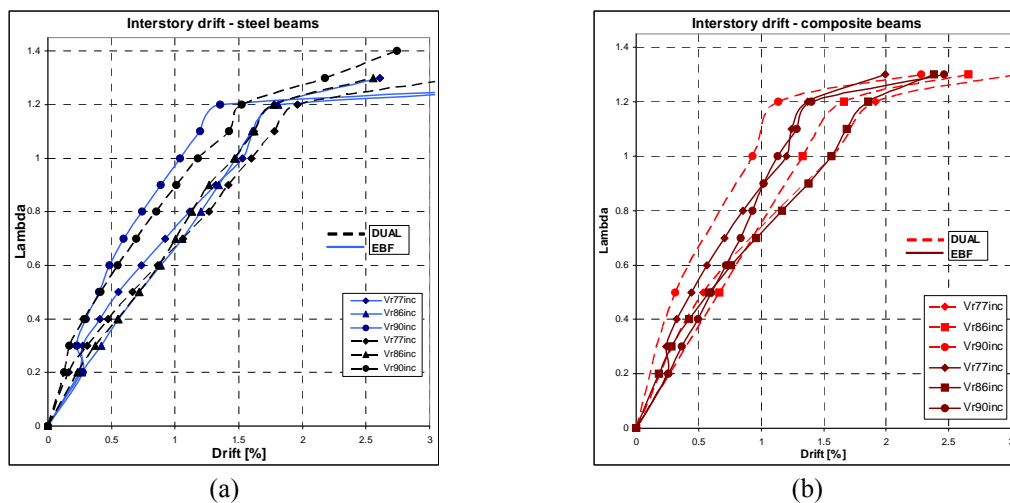


Fig. 19 IDA response representations for the DUAL and EBF 8 story steel and composite structures

factor is equal in this case to the ultimate value of accelerograms multiplier –  $\lambda_u$ . The values listed in Table 3 represent the average values computed for all the seven accelerograms considered for analysis. The exact values of the  $q$  factors for each structure and accelerogram could be found elsewhere (Danku 2011).

The  $q$  values resulted show good agreement with the value used for design ( $q = 6$ ) for EBF and DUAL type frames but for pure steel structures only. These are coherent with the values found by other researchers (Rossi and Lombardo 2007, Degee *et al.* 2010). However, smaller values are found for composite structures. This fact could be explained by the higher rigidity offered by composite beams. Although the ultimate accelerograms multipliers are about the same for steel and composite frames, higher  $\lambda$  values are required for the first plastic hinge in composite beams. Therefore, the overall  $q$  values are smaller than in the case of steel structures.

The values of the seismic efficiency proves a global minimum reserve for all structures (steel and composite) greater than 20%, which could be judged as safe for actual design. The final value of  $\eta$  do not depend on the structural typology (steel/concrete, DUAL/MRF/EBF), but only for the real response under different accelerograms.

#### 4.7 Investigation of overstrength factors

The overstrength  $\Omega$  factors are used in the design of non-ductile elements (columns, for example) and represent the minimum ratio between the loading level of ductile elements under seismic combination conditions and the plastic capacity of the element section (clauses 6.6.3 and 6.8.3 of Eurocode 8). The  $\Omega$  factor should be unique for the whole structure. The usual values of the  $1.1\gamma_{ov}\Omega$  product for design range between 2 and 4. For the structures under consideration, a value of 2.5 was used for EBF, and 3 for MRF. The seismic analyses performed on accelerograms for the equivalent elastic analysis show that the  $\Omega$  values increase from bottom elements to top ones, which means that top dissipation elements are usually not very stressed under seismic

Table 3 Accelerogram multipliers, q factor and structural efficiency

Structure	Configuration	$q_{avg}$	$\eta_{avg}$
F1 DUAL - 4	Steel	5.5	1.4
	Composite	3.9	1.2
F6 DUAL - 12	Steel	5.8	1.4
	Composite	4.9	1.2
F7 MRF - 5	Steel	5.8	1.5
	Composite	5.8	1.5
F5 EBF - 6	Steel	5.9	1.2
	Composite	3.6	1.2
F4 EBF - 8	Steel	6.5	1.3
	Composite	5.8	1.2
F3 DUAL - 8	Steel	5.8	1.4
	Composite	4	1.3

\* Note:  $q_{avg}$  and  $\eta_{avg}$  represent the average values of all earthquake recordings

Table 4 Overstrength factor values

Structure	$\Omega$ - EBF		$\Omega$ - MRF		$\Omega$ - structure		$1.1*\gamma_{ov}*\Omega$	
	steel	composite	steel	composite	steel	composite	steel	composite
F1 DUAL - 4	2.16	2.22	2.83	2.94	2.16	2.22	2.97	3.06
F3 DUAL - 8	1.52	1.55	1.39	1.72	1.39	1.55	1.91	2.13
F6 DUAL - 12	1.57	1.58	1.32	1.39	1.32	1.39	1.81	1.91
F2 EBF - 4	1.52	1.62	---	---	1.52	1.62	2.09	2.23
F5 EBF - 6	1.83	2.07	---	---	1.83	2.07	2.51	2.84
F4 EBF - 8	1.53	1.67	---	---	1.53	1.67	2.11	2.30
F8 MRF - 5	---	---	1.08	1.18	1.08	1.18	1.49	1.62
F8 MRF - 5	---	---	1.04	1.30	1.04	1.30	1.43	1.78

conditions, leading to high values of 7 or 9. However, this conclusion is coherent with the order of formation of plastic hinges. Consequently, minimal values of the overstrength factor  $\Omega$  are always taken from the lower stories.

Table 4 gives the overstrength factor values for the structures under analysis, computed separately where the case for MRF, EBF and overall DUAL values. The smallest values were resulting for MRF with values close to 1.0 both for steel and composite structures. This fact proves the efficiency of RBS solution. The final values of overstrength product  $1.1*\gamma_{ov}*\Omega$  (between 1.5 and 2) is smaller than the values used in design.

However, in the case of simple EBF structures, overstrength factors are higher, the maximum values being 1.8 for steel and 2.1 for composite frames. This leads to average  $1.1*\gamma_{ov}*\Omega$  values of 2.5 for steel structures (identical to the ones prescribed) and 2.8 for composite.

For DUAL frames,  $\Omega$  factors have been computed for both MR's and EBF's. In this situation, the MRF beams are less stressed as compared to simple moment resisting frames, this being proved by higher  $\Omega$  values. On the other hand, smaller values are obtained for EBF of dual frames in comparison to pure EBF. This leads to the conclusion that seismic-induced efforts are redistributed, compared to the case of pure MRF and EBF frames, namely from MRF to EBF. In order to be coherent with modern seismic norms, a single  $\Omega$  factor should be used for the entire structure. Therefore, the lowest  $\Omega$  value should be considered from all the values computed for MR and EB elements. For our applications, the values found could be divided into two cases:

- for low-rise buildings (e.g., 4 storey structures) the  $1.1*\gamma_{ov}*\Omega$  products given in norms are smaller than the obtained values. This could lead to underdimensioned non-ductile elements (columns and braces in this case);
- for medium-rise buildings (8 to 12 storeys) the  $1.1*\gamma_{ov}*\Omega$  product is within the limits of the values used for design.
- The composite frames have greater values for both  $\Omega$  and total  $1.1*\gamma_{ov}*\Omega$  products. However, this is against the existing prescriptions, which guarantees the same values for steel and composite frames.

## 5. Conclusions

The numerical calibration of dissipative component behavior by using ordinary design

computer programs (e.g., SAP2000), may lead to the optimization of the behavior of short link and RBS in dual MRF and EBF, for both steel and composite solutions, which can be further used in wider numerical analyses.

The Incremental Dynamic Analyses (IDA) has proven that structures where the interaction between steel and concrete was modeled have had a different behavior from the bare steel ones. Low-rise steel structures (4 stories, 5 stories) show higher drift and rotation requirements than the similar frames modeled with composite beams. For the high-rise structures, with a higher vibration period, the increase in strength and rigidity induced by the composite effect also leads to smaller rotations in links and RBS. Consequently, in an optimum design, smaller sections could be considered in the case of composite elements, leading to an overall economy in terms of steel.

Numerical results indicate that the main plastic deformation requirements in the case of DUAL (MRF+EBF) structures are to be found mainly in the links (with values around 100 mrad for the design situation) and with some contribution from the RBS (values around 20 mrad for the ULS). From this point of view, the value proposed by EC8-1, § 6.8.2., namely of 80 mrad for the short links in EBF, becomes insufficient for DUAL frames.

The values for the behavior factor  $q$ , obtained for the analyzed steel structures, are close to the prescribed design values (e.g.,  $q = 6$  for DUAL frames), confirming the good dissipation capacity of these systems. It is to be noted that, following numerical analyses, for the composite structures, behavior factors resulted with smaller values than for the same structures with steel beams (e.g., for the DUAL frames, between 4 and 5, with respect to 6).

By analyzing seismic efficiency –  $\eta$ , results showed that the analyzed structures have strength and ductility reserves of about 20-40%, as compared to the design requirements.

## References

- Bosco, M. and Rossi, P.P. (2009), “Seismic behaviour of eccentrically braced frames”, *Eng. Struct.*, **31**(3), 664-674.
- Chao, S-H. and Goel, S.C. (2006), “Performance-based seismic design of eccentrically braced frames using target drift and yield mechanism”, *AISC Eng. J.*, 3rd Quarter, 173-200.
- CSI – Computers and Structures Incorporation (2012), *SAP 2000 Overview*, Online at; <http://www.csiberkeley.com/sap2000>
- Danku, G. (2011) “Study of the development of plastic hinges in composite steel-concrete structural members subjected to shear and/or bending”, Ph.D. Thesis, Politehnica University of Timisoara.
- Degée, H., Lebrun, N. and Plumier, A. (2010), “Considerations on the design, analysis and performances of eccentrically braced composite frames under seismic action”, *Proceedings of SDSS 2010 Conference – Stability and Ductility of Steel Structures*, 337-344.
- Elghazouli, A.Y., Castro, J.M. and Izzuddin, B.A. (2008) “Seismic performance of composite moment-resisting frames”, *Eng. Struct.*, **30**(7), 1802-1819.
- European Committee for Standardization, EN 1998-1 EUROCODE 8 (2003), Design of structures for earthquake resistance, Part 1. General rules, seismic actions and rules for buildings, Brussels, CEN.
- Fajfar, P. (2000), “A nonlinear analysis method for performance-based seismic design”, *Earthq. Spectra*, **16**(3), 573-592.
- Federal Emergency Management Agency (2000), FEMA 356: Prestandard and Commentary for the Seismic Rehabilitation of Buildings, Washington, D.C., November.
- Huang, Y., Yi, W. and Nie, J. (2012), “Seismic Analysis of CFST Frames Considering the Effect of the Floor Slab”, *Steel Compos. Struct., Int. J.*, **13**(4), 397-408.
- Nie, J. and Tao, M. (2012), “Slab spatial composite effect in composite frame systems, I: Effective width for

- ultimate loading capacity”, *Eng. Struct.*, **38**, 171-184.
- Nie, J. and Tao, M. (2012), “Slab spatial composite effect in composite frame systems, II: Equivalent stiffness and verifications”, *Eng. Struct.*, **38**, 185-199.
- Özhendekci, D. and Özhendekci, N. (2008), “Effects of the frame geometry on the weight and inelastic behaviour of eccentrically braced chevron steel frames”, *J. Construct. Steel Res.*, **64**(3), 326-343.
- Plumier, A. (1990), “New idea for safe structure in seismic zone”, *Proceedings of IABSE Symposium on Mixed Structures including New Materials*, 431-436, Brussels, September.
- Prakash, V. and Powell, G. (2012), DRAIN 2DX – computer manual and software, Online at; <http://nisee.berkeley.edu/elibrary/getpkg?id=DRAIN2DX>.
- Ricles, J.M. and Popov, E.P. (1987), *Experiments on Eccentrically Braced Frames with Composite Floors*, Earthquake Engineering Research Center, University Of California, Berkeley, California.
- Romanian Institute of Standardization (2006), P100-1-2006: P100-1 Seismic Design Code, Part I – Design Rules for Buildings, ASRO.
- Rossi, P.P. and Lombardo, A. (2007), “Influence of the link overstrength factor on the seismic behaviour of eccentrically braced frames”, *J. Construct. Steel Res.*, **63**(11), 1529-1545.
- The Regents of the University of California (2012), OpenSees computer code, Online at; <http://opensees.berkeley.edu>
- Vasdravellis, G., Valente, M. and Castiglioni, C.A. (2009), “Dynamic response of composite frames with different shear connection degree”, *J. Construct. Steel Res.*, **65**(10-11), 2050-2061.
- Zona, A., Barbato, M. and Conte, J. (2008) “Nonlinear seismic response analysis of steel–concrete composite frames”, *J. Struct. Eng. ASCE*, **134**(6), 986-997.

BU